Proceedings of the IASS Annual Symposium 2016
"Spatial Structures in the 21st Century"
26–30 September, 2016, Tokyo, Japan
K. Kawaguchi, M. Ohsaki, T. Takeuchi (eds.)

Design of tree-type support structure of free-form shell generated using fractal geometry

Jinglan CUI*, Guangchun ZHOU [a], Makoto OHSAKI [b]

*Department of Architecture and Architectural Engineering, Kyoto University
Kyoto-Daigaku Katsura, Nishikyo, Kyoto 615-8540, Japan
cui.jinglan.63w@st.kyoto-u.ac.jp

[a] Harbin Institute of Technology
[b] Kyoto University

Abstract

Owing to the development of architectural design method and technologies for fabrication and construction, we have more chance to design a complex shape for long-span structures [1]. For realizing a rational form of free-surface, the load path to the support structure is a significant factor. Hence, optimization of support structure is equivalently important as optimization of the shell surface.

Tree-type support structure, first proposed by German architect/engineer Frei Otto in 1960, was applied to Stuttgart airport. Since then, more and more tree-type support structure were built, for instance the London Stansted airport, the Lisbon Oriente station and the Mumbai Tote restaurant. However, the existing tree-type support structures were designed based mainly on aesthetic factor rather than on physical rationality.

The idea of biomimetics [2], which designs artifacts by mimicking the characteristics of organisms like the artificial life [3], is not new; however, recent development of computer technology enabled us to apply it to various fields of engineering including architectural design, construction, planning and environment [4,5].

In order to achieve a tree-type support structure considering the mechanical rationality, various methods have been proposed. Rational tree-type structures were obtained by Kolodziejczyk [6] through 'wet silk model method' for reverse-hanging experiment, and by von Buelow [7] through 'dry silk model method'. Moreover, von Buelow [8] investigated the method that generates rational tree-type structure by utilizing genetic algorithm. Hunt [9] proposed a tree-type structure that transmits loads with axial force only by transforming rigid connections into pins. Cui and Jiang [10] minimized the strain energy of structure using the sensitivity coefficients, and presented a method for simultaneously optimizing the shape, topology and sectional area of skeletal structures including tree-type structures. Among the methods of biomimetics and artificial life, the fractal geometry proposed by Mandelbrot [11] can express the tree shape in nature. The L-system is a typical application of fractal geometry to generate tree-type[12] structures.

In this study, we propose a method of optimizing a tree-type support structure, considering the aesthetic effect, to evolve the structure to a rationalized form. The initial shape is generated using the fractal geometry [13], and the B-spline curve is used to generate the boundaries and cave of the free-form shell. It is shown in the numerical examples that the strain energy of overall structure can be reduced by optimizing the shape of the tree-type structure.

1. Method for generating the shape of a tree-type support structure

We use the Iterative Function System (IFS) of fractal geometry to generate the branches of the tree-type

Copyright © 2016 by <J.L. Cui, G.C. Zhou and M. Ohsaki>
Published by the International Association for Shell and Spatial Structures (IASS) with permission.

structure. IFS is based on affine transformation in the 3-dimensional space. The global coordinate system and the local coordinate system of a member are denoted by (x, y, z) and (x', y', z'), respectively. As indicated in Fig.1, we denote the projection of branch ab to XY plane as $a'b'$. The angle between ab and x-axis and the angle between $a'b'$ and z-axis are denoted by θ_x and θ_z, respectively. The global coordinate (x, y, z) is translated so that its origin coincides with the end point b of branch ab, followed by rotation of θ_x around z-axis, and rotation of θ_z around y-axis, to generate a new local coordinate system (x', y', z'), as shown in Fig 1(b). In this local coordinate system, z'-axis is located in the member direction from point b, and x'-axis exists in the plane formed by branch ab and its projection $a'b'$.

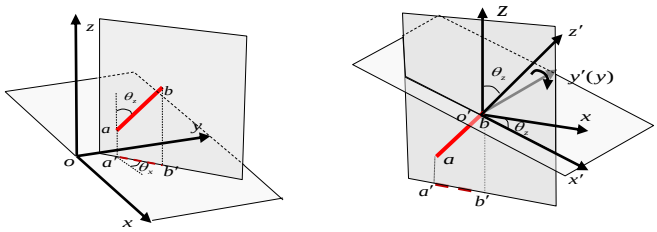

a branch location of all coordinates **b local coordinate of branch end**

Fig.1 Definition of local coordinate system by affine

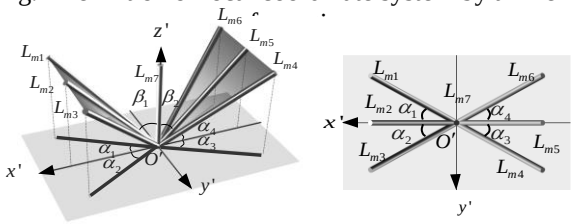

Fig.2 Possible locations of branches

New branches are generated using the local coordinate system (x', y', z'). The branches may exist in positions $Lm1, \ldots, Lm7$, shown in Fig. 2. β_1 and β_2 are the angles between z'-axis and the projection of ($Lm1$, $Lm3$) and ($Lm4$, $Lm6$), respectively, to $x'y'$ plane. The angles between z'-axis and $Lm2$ and $Lm5$ are also β_1 and β_2, respectively. $\alpha_1, \alpha_2, \alpha_3, \alpha_4$, respectively, are the angles between x'-axis and the projection of $Lm1, Lm3, Lm4, Lm6$ to $x'y'$ plane. The projected lines of $Lm2$ and $Lm5$ to $x'y'$ plane are located on x'-axis . The new branch angles $\beta_1, \beta_2, \alpha_1, \alpha_2, \alpha_3, \alpha_4$ are related to the width of the upper part of the tree. To prevent too large angle between branches, we assign β_0 in advance, and compute β_2 from β_1 as

$$\beta_1 + \beta_2 = \beta_0 \tag{1}$$

In addition, the length L and cross-sectional area s of the branch are decreased with the progress of branching by the ratios γ and ρ, respectively as

$$\begin{cases} L^{(k+1)} = \gamma L^{(k)}, & (0 < \gamma < 1) \\ s^{(k+1)} = \rho s^{(k)}, & (0 < \rho < 1) \end{cases} \tag{2}$$

where, *k* is the step number of branching.

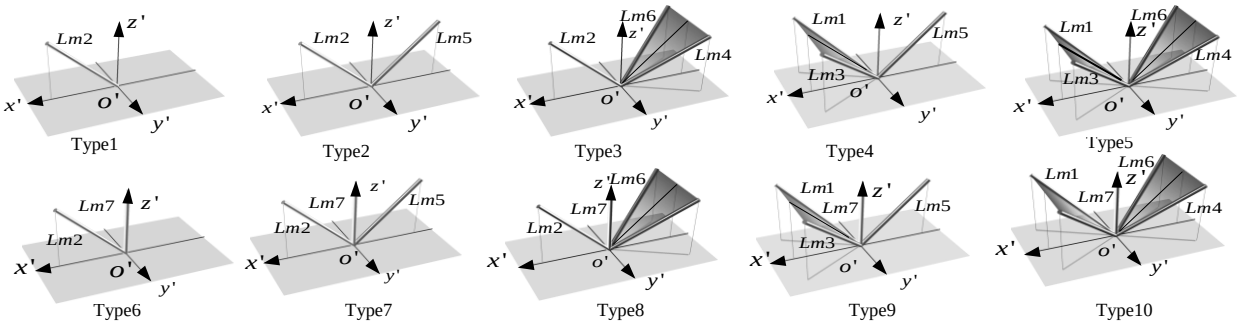

Fig.3 Branch types

The new branch is determined by a combination of *lm*1 to *lm*7; however, the combinations are classified into 10 different types. In five stage branch, for example, if types 3, 4, 4, 5, 3 are applied at the stages 1, 2, 3, 4, 5, respectively, then the tree generation grammar is defined as $A=(3,4,4,5,3)$.

Figure 4 shows a result of eight stage branch with $A=(3,4,4,3,4,4,4,4)$. We can see a realistically imitating natural tree shape. However, simply using the above mentioned methods will lead to a shape with sagging branches. This is beneficial in nature, but is not accepted for a support structure. Therefore, when calculating the angle θ_z between *z*-axis in the global coordinate and *z* '-axis in the local coordinate, β_1 is bounded by $(90^\circ-\theta_Z)$ as

$$\beta_1=\eta(90^\circ-\theta_Z) \qquad (0<\eta<1.0) \tag{3}$$

Figure 5 shows the result using the same grammar as Fig. 4 with the condition (3) so that there is no sagging branch.

Fig.4 An example of tree-type structure

Fig.5 Modified tree-type structure

2. Definition of initial shape of tree-type support structure and free-form shell

We suppose the shape of free-form shell is defined to meet the operating and construction requirements, and only optimize the shape of tree-type support structure. In this section, generation method of initial shape before optimization of the tree-type support structure is described.

2.1. Determination of plane boundary

In order to model the irregular boundary shape, B-spline curves with odd order $(2m-1)$ is extended and used for defining the curve with several intervals. Suppose there are N pieces of closed curves along the inside and outside the boundaries. The i th closed curve has M_i intervals, and each interval is defined as

$$\begin{cases} x(t) = \sum_{i=1}^{N} \sum_{j=1}^{M_i} \sum_{k=S_{ij}}^{T_{ij}} c_k^x B_{k,2m_{ij}}(t) \\ y(t) = \sum_{i=1}^{N} \sum_{j=1}^{M_i} \sum_{k=S_{ij}}^{T_{ij}} c_k^y B_{k,2m_{ij}}(t) \end{cases} \tag{4}$$

where, S_{ij} and T_{ij} are the numbers of first and last basis functions, and $(2m_{ij}-1)$ is the order of basis function of the i *t*h closed curve. c_k^x and c_k^y are the linear combination coefficients of $B_{k,2m_{ij}}(t)$, and $B_{k,2m_{ij}}(t)$ is the B-spline basis function that can be obtained by the recursive formula [14] of de Boor and Cox. For each external boundaries and internal boundaries, we specify the sets (t_k, x_k) and (t_k, y_k), and solve Eq. (4) for the coefficients c_k^x and c_k^y. Finally, equally divide (t_k, t_{k+1}) to determine using Eq. (4) the coordinates of the points, where the nodes of finite element analysis are located.

2.2. Generation of free-form surface shape

The shape of the free-form surface is modeled using the tensor product B-spline surfaces. The order of basis functions in *x*- and *y*-directions are denoted by *m* and *n*, respectively. The number of basis functions $B_{i,2m}(x)$ and $B_{j,2n}(y)$ in *x*- and *y*-directions are denoted by *M* and *N*, respectively. Using the linear combination coefficients $\gamma_{i,j}$, the surface *z*(*x*,*y*) is defined as

$$z(x,y) = \sum_{i=1}^{M} \sum_{j=1}^{N} \gamma_{i,j} B_{i,2m}(x) B_{j,2n}(y) \tag{5}$$

The external boundaries of shell contained in the rectanglular domain is divided into grids on the *xy*-plane. The coefficients $\gamma_{i,j}$ are determined by assigning the height z_{ij} at the point (x_i, y_j) and solving Eq. (5).

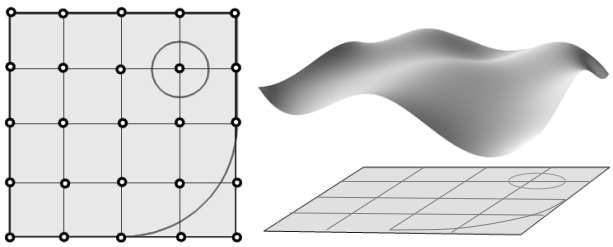

a Setting of plane grid b Surface shape

Fig.6 B-spline surface shape

2.3. Generation of initial shape

For the given initial shape of tree-type support, planar boundary shape, and free-form surface shape, we optimize the shape the tree-type support. Therefore, we obtain the intersection between the branches of tree-type structure and free-form surface. The intersection point is the anchored point to free-form surface.

Then we carry out Delaunay triangulation by specifying the support points of tree structure and nodes on inside and outside boundaries on the *xy*-plane. The points and lines of triangulation are projected onto the shell surface to obtain the triangular mesh for finite element analysis.

3. Optimization problem of structural shape

We optimize the nodal coordinates of the tree-type structure. The vector of design variables is denoted $\mathbf{X}$, which consists of all variable coordinates of nodes. The objective function is the total strain energy of tree-type structure and surface under vertical live load and self-weight. Let $\mathbf{K}(\mathbf{X})$, $\mathbf{U}(\mathbf{X})$, and $\mathbf{F}(\mathbf{X})$ denote the stiffness matrix of whore structure with respect to global coordinates, the displacement vector, and the load vector, respectively. The stiffness equation is written as

$$\mathbf{K}(\mathbf{X})\mathbf{U}(\mathbf{X}) = \mathbf{F}(\mathbf{X}) \tag{6}$$

Strain energy C can be calculated from

$$C(\mathbf{X}) = \frac{1}{2}\mathbf{U}(\mathbf{X})^T \mathbf{K}(\mathbf{X})\mathbf{U}(\mathbf{X}) \tag{7}$$

The optimization problem is formulated as

$$\begin{cases} \text{find} & \mathbf{X} \\ \text{min.} & C(\mathbf{X}) \\ \text{subject to} & \mathbf{X} \subset \Omega_0 \end{cases} \tag{8}$$

where, Ω_0 is the feasible region of $\mathbf{X}$.

3.1. Sensitivity coefficients of strain energy

The stiffness matrix of the curved shell structure and frame structure are composed of plane triangular elements and beam elements represented, respectively, by $\mathbf{K}_s$ and $\mathbf{K}_h$; i.e.,

$$\mathbf{K} = \mathbf{K}_s + \mathbf{K}_h \tag{9}$$

The coordinates of support points of the tree-type structure are fixed, and the support points on the surface are constrained to move only on the surface. Therefore, variable vector is divided into free nodes $\mathbf{X}^F$ and constrained nodes $\mathbf{X}^C$. Only the beam elements are related to the free nodes; however, both plane triangular elements and beam elements are related to the constrained nodes.

The sensitivity coefficients d_{ix}^F, d_{iy}^F, d_{iz}^F of strain energy with respect to the coordinates x_i^F, y_i^F, z_i^F of the i th free node, respectively, are expressed as

$$\begin{cases} d_{ix}^F = -\dfrac{1}{2}\mathbf{U}^T \dfrac{\partial \mathbf{K}_h}{\partial x_i^F}\mathbf{U} \\ d_{iy}^F = -\dfrac{1}{2}\mathbf{U}^T \dfrac{\partial \mathbf{K}_h}{\partial y_i^F}\mathbf{U} \\ d_{iz}^F = -\dfrac{1}{2}\mathbf{U}^T \dfrac{\partial \mathbf{K}_h}{\partial z_i^F}\mathbf{U} \end{cases} \tag{10}$$

However, the differentiation of stiffness matrix is carried out only for equations related to the i th free node.

z-coordinate of a constrained node is a function of x- and y-coordinates. The sensitivity coefficients d_{ix}^c, d_{iy}^c of strain energy with respect to the coordinates x_i^C, y_i^C of the i th constrained node, respectively, are expressed as

$$\begin{cases} d_{ix}^{c} = -\dfrac{1}{2}U^{T}(\dfrac{\partial K}{\partial x_i} + \dfrac{\partial K}{\partial z_i}\cdot\dfrac{\partial z_i}{\partial x_i})U \\ d_{iy}^{c} = -\dfrac{1}{2}U^{T}(\dfrac{\partial K}{\partial y_i} + \dfrac{\partial K}{\partial z_i}\cdot\dfrac{\partial z_i}{\partial y_i})U \end{cases} \tag{11}$$

Substituting Eq. (5) into Eq. (11), we obtain d_{ix}^{c}, d_{iy}^{c} as

$$\begin{cases} d_{ix}^{c} = -\dfrac{1}{2}U^{T}[\dfrac{\partial K}{\partial x_i} + \dfrac{\partial K}{\partial z_i}\sum_{k=1}^{M}\sum_{j=1}^{N}\gamma_{k,j}\dfrac{\partial B_{k,2m}(x)}{\partial x_k}B_{j,2n}(y)]U \\ d_{iy}^{c} = -\dfrac{1}{2}U^{T}[\dfrac{\partial K}{\partial y_i} + \dfrac{\partial K}{\partial z_i}\sum_{k=1}^{M}\sum_{j=1}^{N}\gamma_{k,j}\partial B_{k,2m}(x)\dfrac{\partial B_{j,2n}(y)}{\partial y_k}]U \end{cases} \tag{12}$$

3.2. Optimization method of tree-type support structure for free-form surface

Using the sensitivity coefficients of strain energy with respect to the nodal coordinate vector $\mathbf{X}$, the gradient $\nabla C(\mathbf{X})$ can be obtained, and the optimal solution is found using the steepest descent method.

From the solution $\mathbf{X}^k$ of step *k*, the solution is updated using step length λ_k as follows:

$$\mathbf{X}^{k+1} = \mathbf{X}^k + \lambda_k \nabla C(\mathbf{X}) \tag{13}$$

The step size is determined by the golden section. The termination condition is given as

$$\left|C^{k+1} - C^k\right| \le \varepsilon \quad \text{or} \quad \left|\alpha_{\max}^{k+1}\right| \le \varepsilon \tag{14}$$

where ε is a sufficiently small value, herein set $\varepsilon = 1.0\times10^{-8}$.

4. Examples

Figure 7(a) shows the $40.0m \times 40.0m$ square region of designing a free-form shell. The shell surface is pin-supported to stiff columns at A, B, and C, and support by a tree-type structure with pipe section at

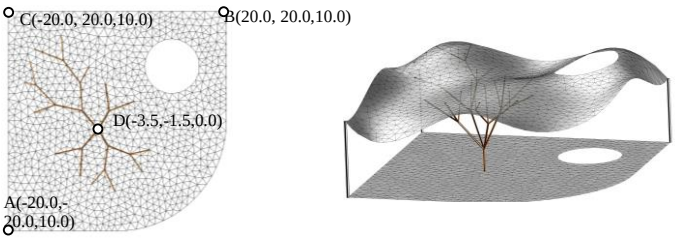

a Triangulation of grid b Initial shape

Fig.7 Formation of initial shape

D. We use the grammar $A_m = (5,4,4,4,4,4)$ to generate the shape of a tree structure. The length and diameter of the main pole (the lowest vertical pole) are $L_c = 3.5m$ and $D_c = 25.0cm$, respectively. The standard length and diameter are $L_0 = 6.0m$ and $D_0 = 20.0cm$.

Moreover, the reduction rates of branch length and area are γ=0.7 and ρ= 0.8, respectively, and the parameter of the branch is η =0.7. The thickness of the pipe is 0.01m, and the material is steel with elastic modulus 210GPa and Poisson's ratio 0.3. The thickness of upper free-form surface is 0.01m, and the material is reinforced concrete with elastic modulus 30GPa and Poisson's ratio 0.2.

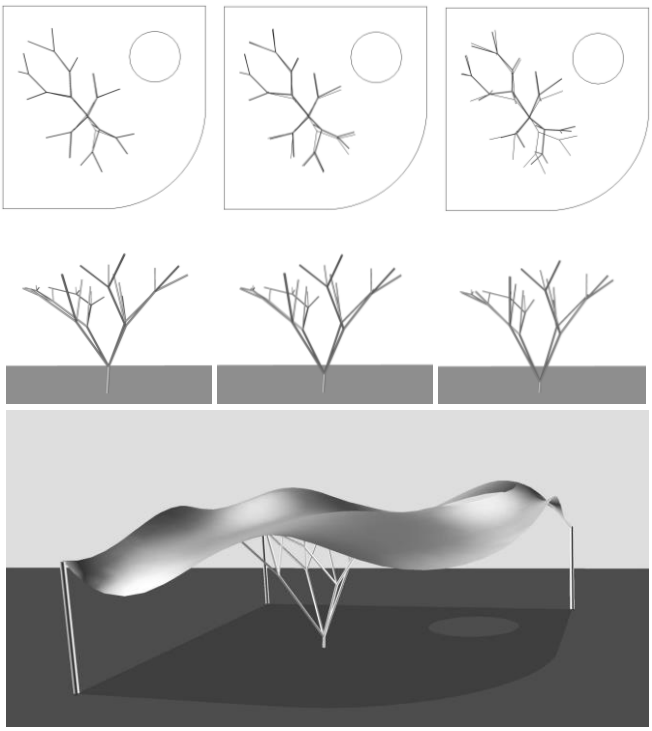

Fig.8 Tree-type structure evolution stereogram

Figure 8 shows the optimal shape obtained from Fig. 7. The evolution process is shown in the plan and elevation in Fig. 8, where the solid line is the position of initial shape of the tree-type structure, and dotted line is the shape in the evolution process. As we can be seen from Fig. 8, the locations of free and constrained nodes of the optimal solution are far from the intial locations; the lowest branch connecting to the base of the optimal shape is much shorter than that of the initial shape.

Figure 9(a) shows the reduction ratio of the strain energy of whole structure and tree structure in evolution process. The strain energy of the tree structure rapidly decreases to 40% of the initial structure at step 20, and further decreases to 30%, while the strain energy of whole structure decreases only to.

Figure 9(b) shows the reduction ratios of the strain energy related to axial force and bending moment, which are hereafter simply called axial force and bending moment. As a result of optimization, the axial force reduces to 82% of the initial value, while the bending moment reduces to 42%. Bending moment changes much greater than the axial force, especial in the first 15 steps of optimization.

Figure 9(c) shows the reduction ratios of strain energy corresponding to membrane stress and bending stress, which are hereafter simply called membrane stress and bending stress, of upper free-form surface. By optimizing of nodal locations of tree-type structure, the membrane stress of upper surface reduces to 75% of the initial value, while bending stress decreases to 51%. This way, the deformation of the upper surface is improved by optimizing the shape of lower structure.

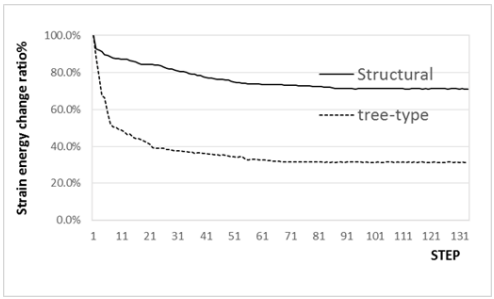

a Strain energy

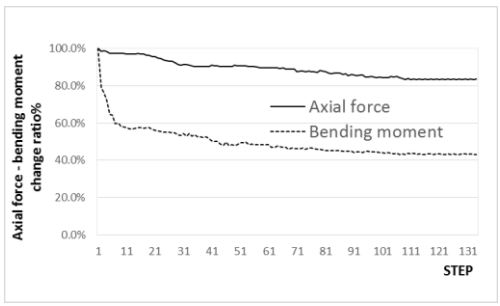

b Tree-type structure

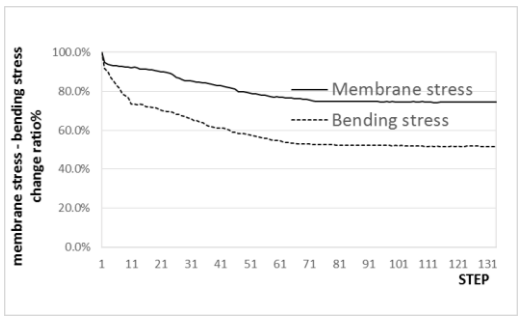

c Upper free-form surface

Fig.9 Change of mechanical properties

The application of fractal geometry to generate tree-type support structure of the free-form surface shell is very effective to design a mechanically rational structure. Furthermore, the tree-type support structure reduces the bending deformation to generate a rational load path dominated by axial force to the base. In the early stage of optimization, minor adjustments of nodes can significantly improve the mechanical properties.

5. Conclusion

The method of shape generation of supporting structure of free-form surface shape has been presented by using fractal geometry. The complex shape of boundary and interior region of upper free-form shell is modelled using B-spline curves and surfaces.

A method has also been presented for modelling a realistic tree shape using IFS based on affine transformation in the 3-dimensional space. The branching types are classified into 10 types, which are combined to define the shape generation grammar. The formulas have been derived for sensitivity analysis of total strain energy with respect to the coordinates of nodes of the tree-type structure, which are constrained on the B-spline surface.

It has been demonstrated in the numerical example that optimization of the tree-type support structure reduces the bending deformation of whole structure generate a rational load path dominated by axial force to the base. In the early stage of optimization, minor adjustments of nodes can significantly improve the mechanical properties.

The method presented in this paper is construction intentions, moreover, full account of the optimization methods under various boundary conditions, not just the mechanics and rational of a structure, but also taking the emotional elements into account, we look forward to help in the actual building design.

References

[1] S. Adriaessens, P. Block, D. Veenendaal and C. Williams (Eds.), Shell Structure for Architecture, Routledge, 2014.

[2] A. Bejan: Shape and Structure from Engineering to Nature, Cambridge University Press, 2000.

[3] E. Thro, Artificial Life Explorer's Kit, Sams Publishing, 1993.

[4] A. Bejan, Shape and Structure, From Engineering to Nature, Cambridge University Press, 2000.

[5] P. Gruber, Biomimetics in Architecture, Springer, 2010.

[6] M. Kolodziejczyk: Verzweigungen mit Fäden, Einige Aspekte der Formbildung mittels Fadenmodellen. Verzweigungen, Natürliche Konstruktionen - Leichtbau in Architektur und Natur., pp. 101-126, 1992.4

[7] P. von Buelow: Following a thread: a tree column for a tree house, Proc. IASS Symposium, Beijing, 2006.

[8] P. von Buelow: A geometric comparison of branching structures in tension and compression versus minimal paths, Proc. IASS Symposium, Venice, 2007.

[9] J. Hunt,W. Haase and W. Sobek: A design tool for spatial tree structures, J. Int. Assoc. Shell and Spatial Struct.,Vol. 50(1), pp. 3-10, 2009.

[10] C.-Y. Cui and B.-S. Jiang: A morphogenesis method for shape optimization of framed structures subject to spatial constraints, Eng. Struct., Vol. 77, pp. 109–118, 2014.

[11] B. B. Mandelbrot, Fractals: Form, Change, and Dimension, W. H. Freeman & Company, 1977.

[12] P. Prusinkiewicz and A. Lindenmayer, The Algorithmic Beauty of Plants, Springer-Verlag, 1990.

[13] C. Bovill, Fractal Geometry in Architecture and Design, Birkhäuser, 1996.

[14] G. Farin, Curves and Surfaces for CAGD, Morgan Kaufmann Publishers, 1999.